Available online www.ejaet.com

European Journal of Advances in Engineering and Technology, 2018, 5(12): 978-995

Research Article ISSN: 2394 - 658X

Voltage and Power Control of Turbo-Generator System using Model Predictive Control and Fractional Order PID Controller

Mahmoud Elshenawy[1], Helmy Elzoghby[2], Mohey Bahgat[3] and A.M.Abdelghany[4]

[1.2.3]Department of Electrical Power and Machines Faculty of Engineering, Helwan University, Cairo, Egypt
[4]on leave for 6 october university, cairo - Originally Department of Electrical Power and Machines Faculty of Engineering, Helwan University, Cairo, Egypt
Engrmahmoud55@yahoo.com, mahmoudelshenawy@h-eng.helwan.edu.eg

---

ABSTRACT

Power system stability and control requirements have been considerably affected by the steady increase in system interconnections, large rating for individual generating units and high transmission voltage. This research presents the model predictive control (MPC) as enormous control technique to cope with the non-linearity, uncertainty and the stabilizing of terminal voltage and power problems of the turbo-generator plant. In recent papers, the parameters of the MPC are tuned based on designer expertise and trial-error technique which may lead to unacceptable performance. This research is interested in the optimal approach of the MPC based on imperialist competitive algorithm (ICA), MPC based on genetic algorithm (GA) and fractional order PID (FOPID) based on GA. The ICA as enormous optimization techniques toselect the optimal parameters of the MPC. Furthermore, a comparison between the ICA-based MPC, GA-based MPC and GA-based FOPID is investigated over a vast running cases with multiple disturbances and robustness study in the case of system parameters uncertainties to validate the effectiveness of the proposed technique.

.

Key words: Model predictive controller (MPC), fractional order PID controller, imperialist competitive algorithm (ICA), genetic algorithm (GA), Turbo-Generator system

---

–

NOMENCLATURE

$\delta^{\bullet}$	Rotor Angular Speed
δ	Rotor angle
H	Inertia constant
P_t , Q_t	Terminal active and reactive power at infinite bus bar
Vf_d	Filed voltage
V_t	Terminal voltage
V_b	Infinite- bus bar voltage
Ψ_f	Field flux linkage
Ψ_d, Ψ_q	d-axis and q-axis stator flux linkages
Ψ_{kd}, Ψ_{kq}	d-axis and q-axis damper winding flux linkages
I_d, I_q	d-axis and q-axis stator currents
I_{kd}, I_{kq}	d-axis and q-axis damper winding currents
X_f	Self-reactance of field winging
X_d, X_q	Synchronous reactance in d-axis and q-axis circuit
X_{kd}, X_{kq}	Self-reactance in d-axis and q-axis of the damper winding
X_{ad}	Reactance between armature and field winding

X_e	Transformer and line reactance
R_e	Transformer and line resistance
R_a	Stator resistance
R_f	Field resistance
R_{kd}, R_{kq}	Resistance of d-axis and q.-axis damper winding
V_d, V_q	Stator voltage in d-axis and q-axis
V_{kd}, V_{kq}	Damper winding voltage in d-and q- axis circuits
$p\ (\ )$	The operator { d/dt}
ω_o	Angular frequency of infinite bus bar
ω	Angular frequency of the rotor
T_e	The electric torque
T_m	Mechanical Torque of generator shaft
μ_{hp}	Steam flow of high pressure
μ_{rh}	Steam flow of reheater
μ_{ip}	Steam flow of intermediate pressure
μl_p	Steam flow of low pressure
μ_q	Governor and interceptor valve positions
τ_{lp}	Time constant of low pressure stage
τ_{ip}	Time constant of intermediate pressure stage
τ_{rh}	Time constant of reheater
τ_{hp}	Time constant of high pressure stage
τ_{iv}	Time constant of interceptor valve
τ_{mv}	Time constant of main valve
P_o	Boiler steam pressure
F_{hp}	Power fraction from high pressure stage
F_{ip}	Power fraction from intermediate stage
F_{lp}	Power fraction from low pressure stage

INTRODUCTION

The increasing complexity of advanced electrical girds has a substantial exertion from researchers towards the advancement of improved techniques of operation and control. The performance of controllers has been facilitated by recent progress in technology, such as fast turbine valving [1], fast acting circuit breakers and thyristor excitation systems [2]. Fast excitation systems have suitable controllers to be investigated which force a rapid change of field voltage in either direction. Therefore, rotor oscillations due to disturbances are quickly damped. The advent of electro-hydraulic governors with fast turbine valving, giving simultaneous operation of the inlet and intercept valves, has considerably altered the concepts of turbine control [3]. In recent, the feedback control is used to stabilize the terminal voltage and terminal power of turbo-generators. In some situation, only the control is carried out on the excitation, and in others, the control includes both excitation and power. The nonlinear system equations of the turbo-generator system are linearized at a specific operating condition, and a linear optimal control theory is applied to determine the digital controller parameters. The utilizing of linear control theory relies on accurate reduced-order linear models of turbo-generator dynamics is founded in [5-7]. In these papers, the models have been considered by applying system identification. The first group has utilized the state formulation to represent the turbo-generator by linearized models. The other group formulated these models utilizing the output prediction equation, utilizing output variables only. Accordingly, the optimal controller gains have been determined by utilizing the linear control theory [8-11]. These optimal controllers get a suboptimal response at any other operating condition because of the non-linearity of the turbo-generator system, which limits the validity of linear models to small perturbations about a particular set of operating conditions. In addition, the uncertainty of the turbo-generator parameters for operating condition changes. All these techniques fail to give an acceptable response due to the nonlinearity of the system. In [10-11], several methods have been suggested to obtain appropriate solutions to this problem. One of these solutions for the nonlinearity problem of the turbo-generator is adaptive models related to control of generator terminal voltage and terminal power. The basic idea of such methods is to state definitely, by optimal design of two controllers that can be utilized through the optimization algorithms. These algorithms are applied to determine the controller parameters to minimize an objective function and obtain the optimal parameters for every controller. Also, the use of these approaches improves the stabilization of both the terminal voltage and the terminal power of the turbo generator system. For the two main problems of the conventional controllers, fuzzy logic controller (FLC) and neurofuzzy logic controller are being facilitated [12-14] butthe model predictive control is being utilized for the following reasons: this technique is very simple as it relies on the input/output values only neglected to the nonlinearity of the system, mathematical equations or system parameters [15-20]. However, the prediction horizon, control horizon, sample time and control weight factor of the MPC need appropriate optimization to get a better controller performance. The aim of this work is the optimal design of the MPC based on ICA for the stabilizing of voltage and power problems of turbo-generator system. The ICA is proved as a powerful optimization technique [21-23]. The MPC based on ICA is compared with the MPC based on GA and the fractional order PID (FOPID) controller based on GA. Furthermore, incorporated transport short circuit and mechanical and electrical variation are considered. The comparison has been investigated under various disturbances. In addition, a robustness test is applied to confirm the effectiveness of the proposed controller versus system parameters uncertainties.

SYSTEM MODELLINGANDDESCRIPTION

Turbo-generators are highly nonlinear system with varying dynamic characteristics due to the fluctuations of operating conditions .Thus, the generator terminal voltage and output power must be adjusted to be in the permissible limits. The control of turbo-generators is represent an important issue for confirm the stability and reliability of the power system. Optimal and adaptive controllers for the generator exciter and turbine governor, designed to control the turbo-generator and turbine performance during disturbances, may be applied to the turbo-generator system. Also, the controllers will extend the transient and steady state stability boundaries. The studied system contains a turbo-generator unit connected to the infinite bus by a transformer and two transmission lines in parallel. Figure 1 describes the schematic diagram of the turbo-generator system. The equations of the non- linear model of the synchronous generator can be expressed in state-space form as follows:

$S^{\cdot} = f(s.u)$, where u = E_{fd}

The state vector (S) is:

$$S = [\,\delta \;\; p\delta \; \psi_{fd} \psi_d \psi_{kd} \psi_q \psi_{kq}\,] \quad (1)$$

And

$$pS_1 = S_2 \quad (2)$$
$$pS_2 = C_1 T_m + S_4(C_2 S_6 + C_3 S_7) + S_6(C_4 S_3 + C_5 S_5) + C_6 S_2 \quad (3)$$
$$pS_3 = C_7 E_{fd} + C_8 S_3 + C_9 S_4 + C_{10} S_5 \quad (4)$$
$$pS_4 = C_{11}\sin(S_1) + C_{12} S_3 + C_{13} S_4 + C_{14} S_5 + S_6 + S_2 S_6 \quad (5)$$
$$pS_5 = C_{15} S_3 + C_{16} S_4 + C_{17} S_5 \quad (6)$$
$$pS_6 = C_{11}\cos(S_1) + C_{18} S_6 + C_{19} S_7 - \omega_o S_4 - S_2 S_4 \quad (7)$$
$$pS_7 = C_{20} S_6 + C_{21} S_7 \quad (8)$$

The state vector of the state-space model of a steam turbine is:

$$[S_8 S_9 S_{10} S_{11} S_{12} S_{13}]^T = [\mu_{hp} \mu_{rh} \mu_{ip} \mu_{lp} Y_{mv} Y_{iv}]^T \quad (9)$$

And

$$P\mu_{hp} = (P_o Y_{mv} - \mu_{hp}) / \tau_{\boldsymbol{hp}} \quad (10)$$
$$P\mu_{rh} = (\mu_{hp} - \mu_{rh}) / \tau_{\boldsymbol{rh}} \quad (11)$$
$$\mu_{ip} = (\mu_{rh} Y_{iv} - \mu_{ip}) / \tau_{\boldsymbol{ip}} \quad (12)$$
$$P\mu_{lp} = (\mu_{ip} - \mu_{lp}) / \tau_{\boldsymbol{lp}} \quad (13)$$
$$Py_{mv} = (\mu_g - Y_{mv}) / \tau_{\boldsymbol{mv}} \quad (14)$$
$$Py_{iv} = (\mu_g - Y_{iv}) / \tau_{\boldsymbol{iv}} \quad (15)$$
$$T_m = F_{hp}\mu_{hp} + F_{ip}\mu_{ip} + F_{lp}\mu_{lp} \quad (16)$$

The thirteen order nonlinear turbo-generator model is defined by combining the equations 2 to 8 as a representative of the generator and equations 10 to 15 as a representative of the steam turbine.

And the electric equations are:

$$V_{td} = V_b\, sin(\delta) + R_e I_d - X_e I_q \quad (17)$$
$$V_{tq} = V_b\, cos(\delta) + R_e I_q + X_e I_d \quad (18)$$
$$V_t^2 = V_{td}^2 + V_{tq}^2 \quad (19)$$
$$I_t^2 = I_d^2 + I_q^2 \quad (20)$$
$$P_t = V_{td} I_d + V_{tq} I_q \quad (21)$$

And the direct current equations are:

$$\begin{bmatrix} Ifd \\ Id \\ Ikd \end{bmatrix} = \begin{bmatrix} Y11 & Y12 & Y13 \\ Y21 & Y22 & Y23 \\ Y31 & Y32 & Y33 \end{bmatrix}^{-1} \begin{bmatrix} \Psi\mathrm{fd} \\ \Psi\mathrm{d} \\ \Psi\mathrm{kd} \end{bmatrix} \quad (22)$$

And the quadrature current equations are:

$$\begin{bmatrix} Iq \\ Ikq \end{bmatrix} = \begin{bmatrix} D11 & D12 \\ D21 & D22 \end{bmatrix}^{-1} \begin{bmatrix} \Psi\mathrm{q} \\ \Psi\mathrm{kq} \end{bmatrix} \quad (23)$$

All constants are defined in the Appendices.

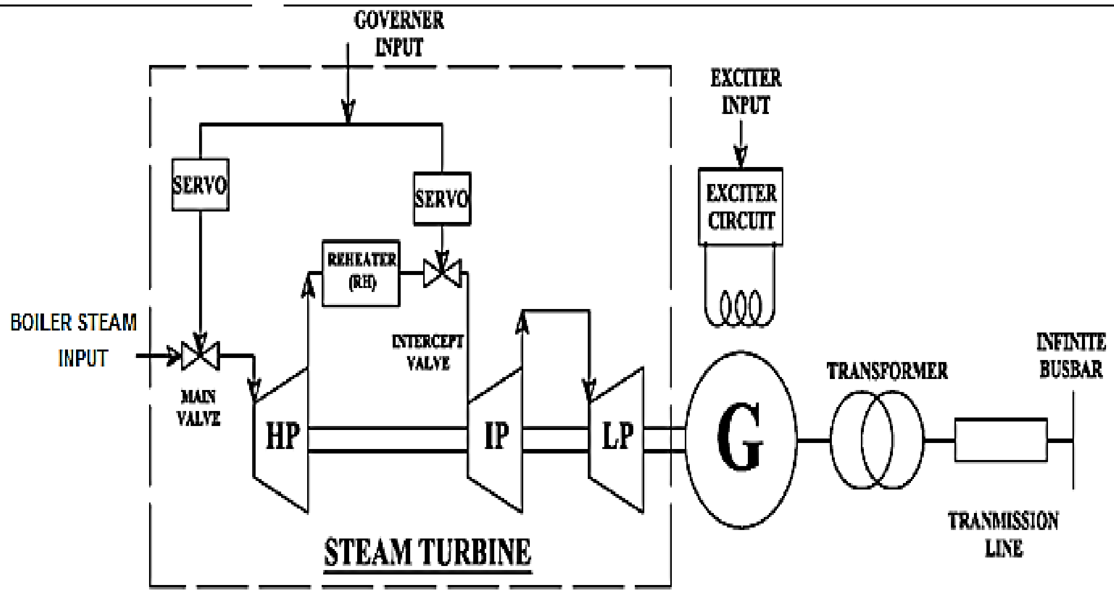

Fig. 1 Schematic Diagram of Turbo-Generator System

And A MATLAB simulation program was developed to study the turbo-generator behavior can be shown from Fig. 2 to Fig. 7.

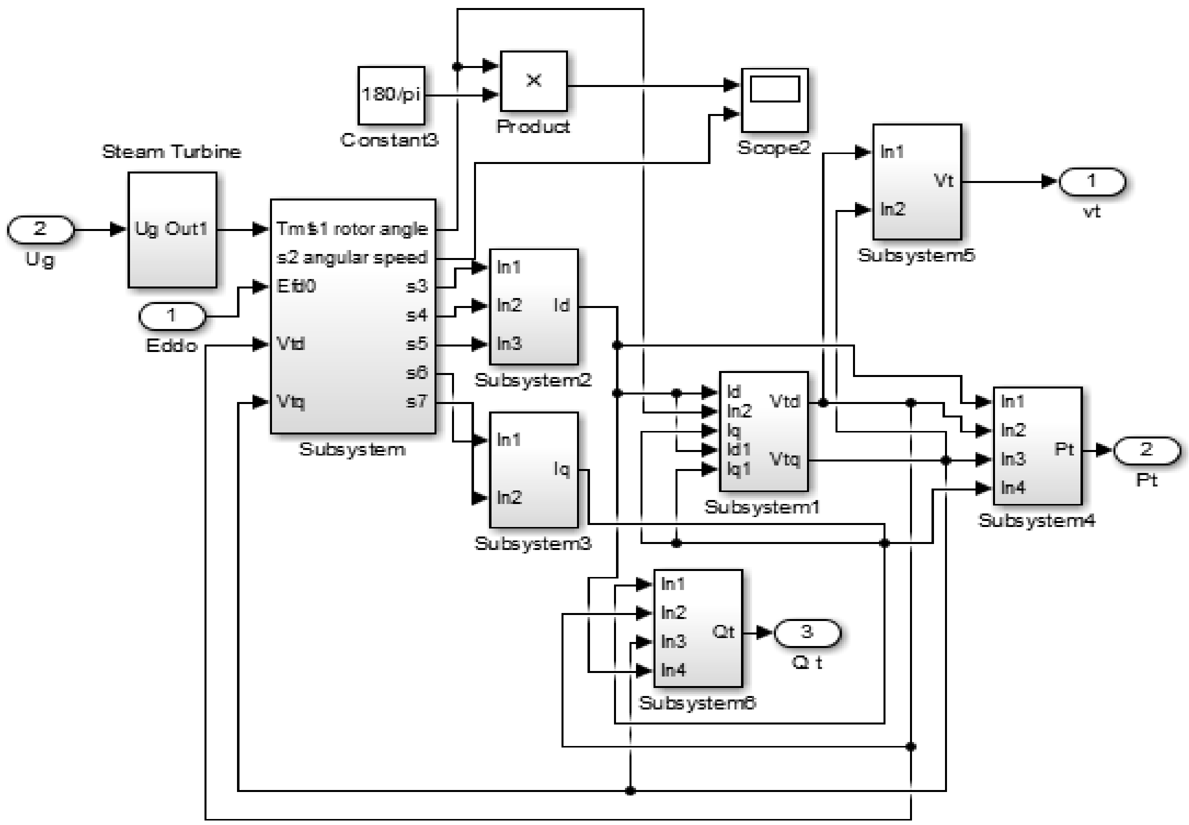

Fig. 2 Turbo-GeneratorSub-Model

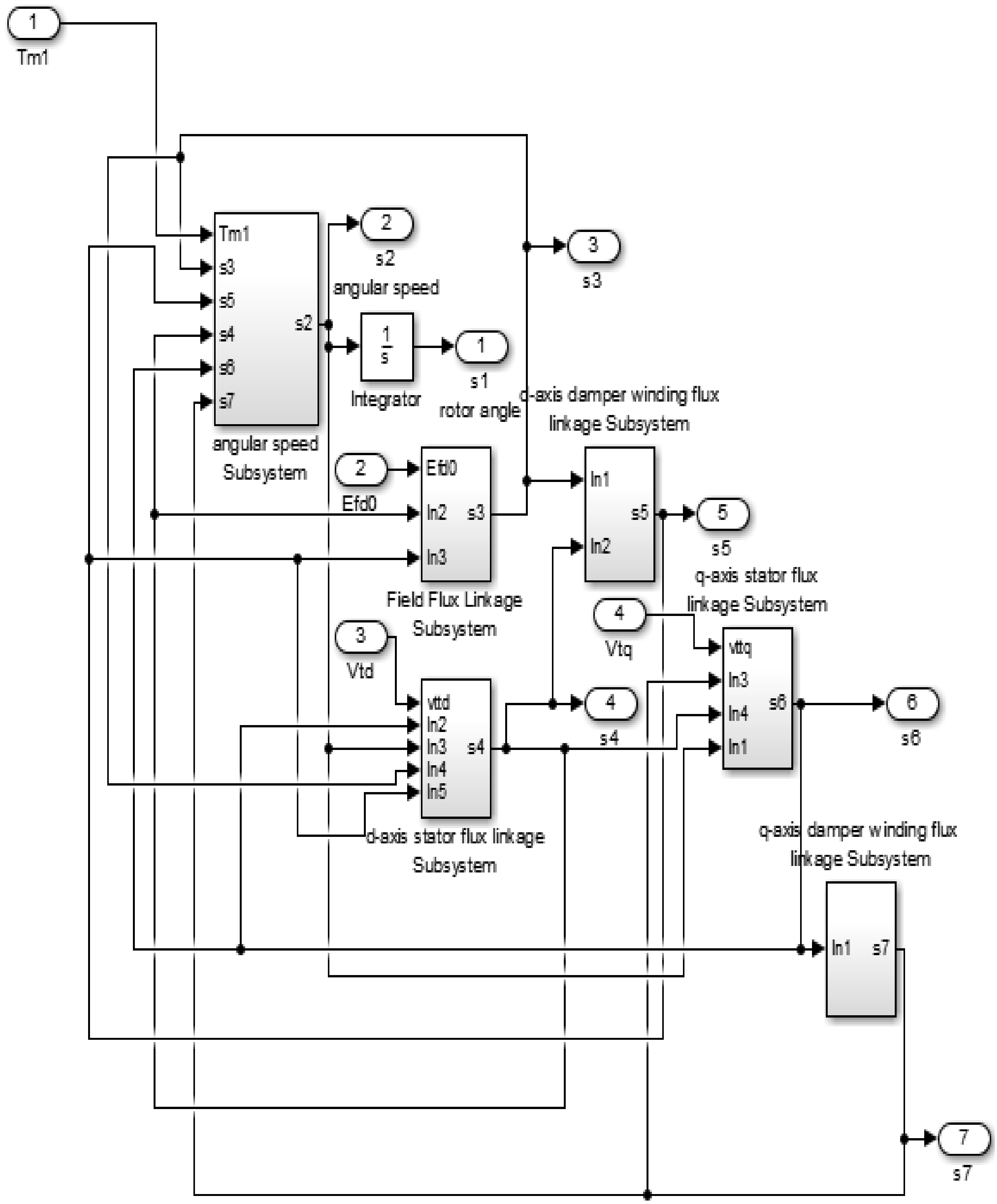

Fig. 3 7th Order |Sub-Model of Synchronous Generator

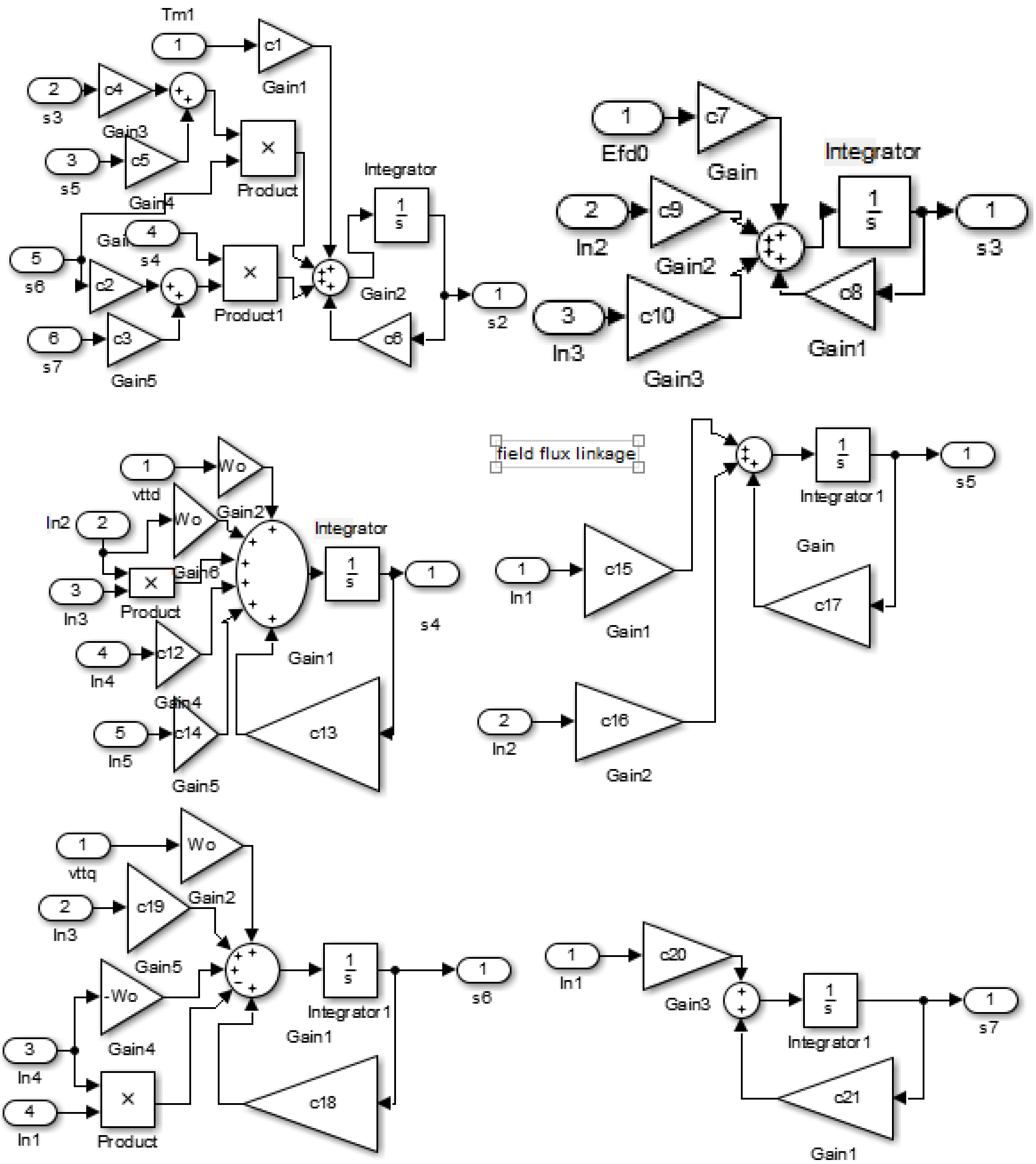

Fig. 4 S2-S7 Sub-Models

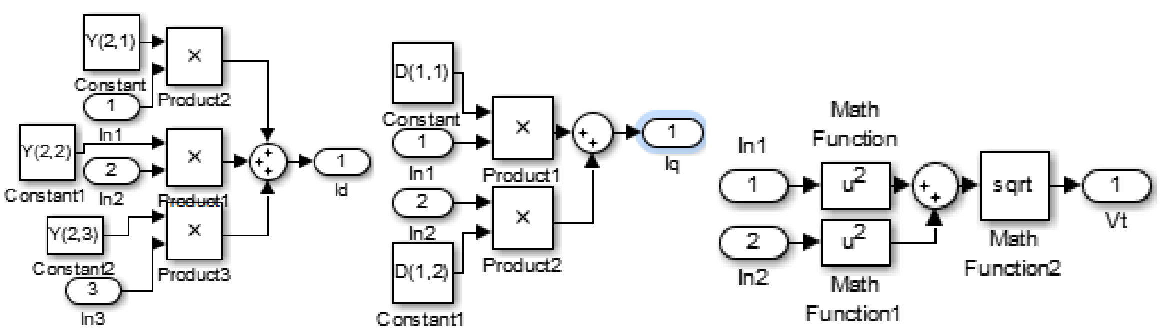

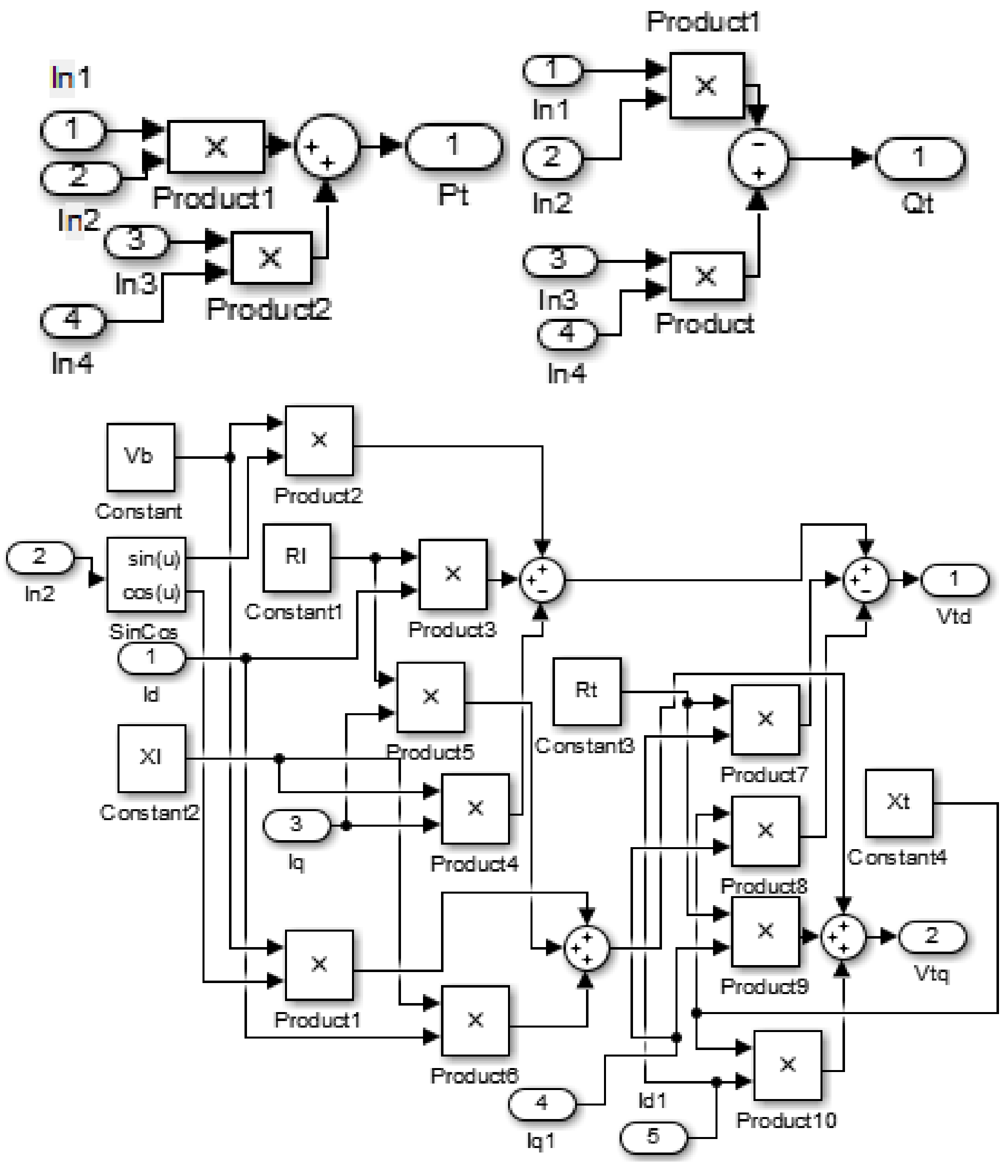

Fig. 5 The Electric Equations Sub-Models

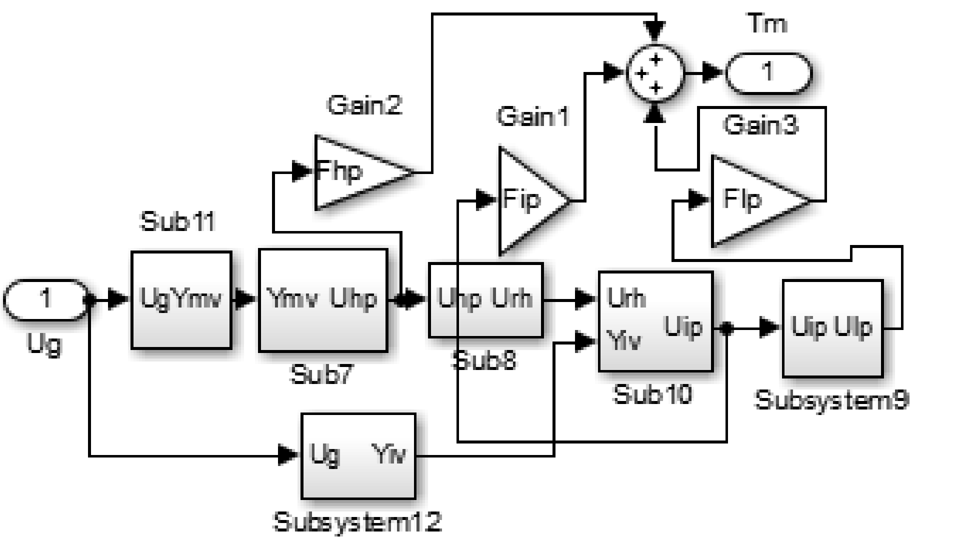

Fig. 6 Turbine simulation and Mechanical Torque sub-model

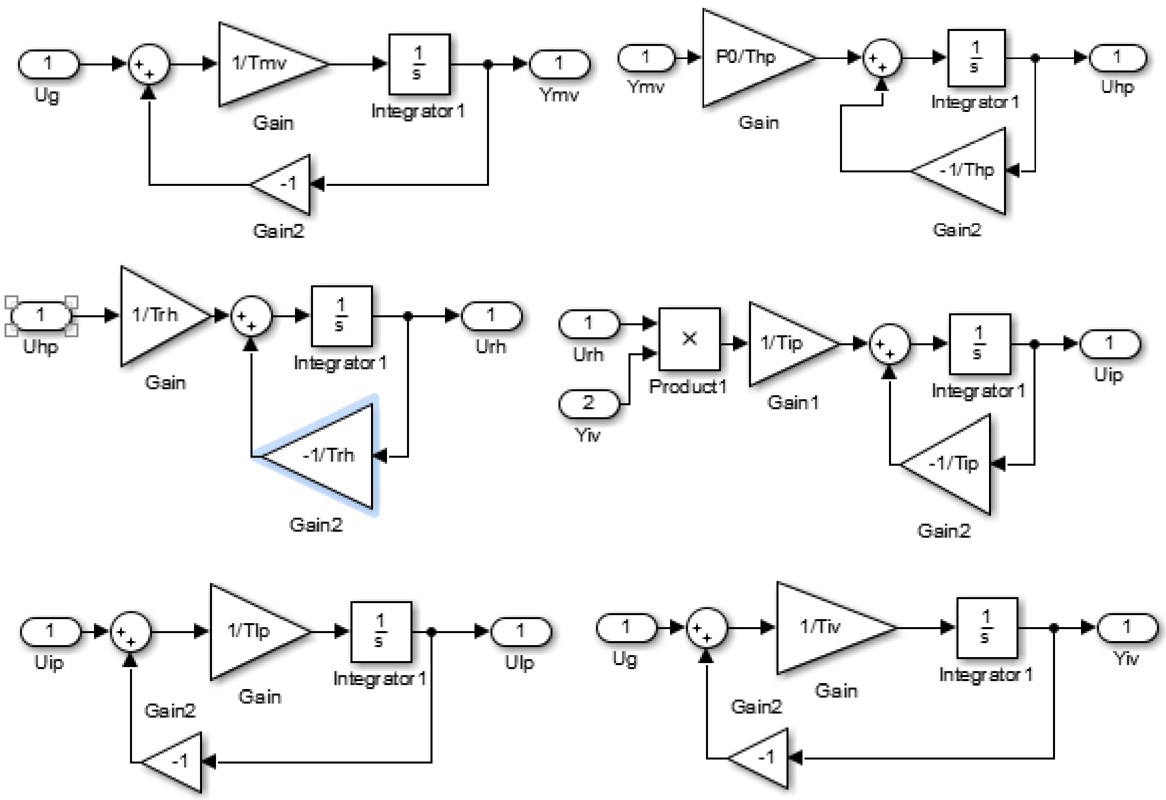

Fig. 7 S8-S13 Sub-models

THEORYOF MPC

The general MPC scheme has two basic units, the first is the prediction unit and the other is the controller unit, as cleared in Fig. 8. The prediction unit predicts the future control action to the system over a finite prediction horizon. The prediction of the control signal is carried out according to the present system output and the disturbances. Thus, the control unit utilizes the predicted output in order to minimize the control objective with considering system constraints. The objective of the optimization mixes the minimization of the contrast between the predicted output and the reference signal, and the control action submitted to satisfied requirements. The feasibility of the MPC is shown to be equal to the optimal control [15-17]. It shows its principles quality in its computational convenience, practical applications, compensation for time delays, handling of constraints, and potential for the future increase of the technique. At every control step, the principal contribution to the optimal arrangement is applied in the plant, and the whole estimation is repeated at each control steps. The cause of taking new estimations at every time step is to adjust the unmeasured disturbances and the inaccuracy of model, both of which cause the process output to be not quite the same as the predicted output [18-20]. The control operations at each prediction step are shown in Fig. 9.

The operation of MPC is applied at the k-th sampling instant. The sampling takes this form 0, Ts, 2Ts, 3Ts, .., kTs, when the MPC starts at time t=0 , Where , Ts is the sample time and K is the current sample. The predicted control signal and the predicted output are accounted according to the minimizing of the following objective function:

$$z = \arg\min_{u} \sum_{i=1}^{P} [Q(r_{k+i} - \hat{y}_{k+i})^2 + R(\Delta u_{k+i-1})^2] \tag{24}$$

Such that,

$$u_{\min} \le u_{k+i} \le u_{\max}$$

$$y_{\min} \le \hat{y}_{k+i} \le y_{\max}$$

$$|\Delta u_{k+i}| \le \Delta u_{\max}$$

Where Q and R are non-negative weights. The MPC accounts the control moves over a control horizon M, where 1≤M≤P.

Each MPC require a proper adjustment of the T_s, Q, R, M, and P to give an acceptable performance so this paper introduces the ICA for the optimal optimizing of MPC parameters.

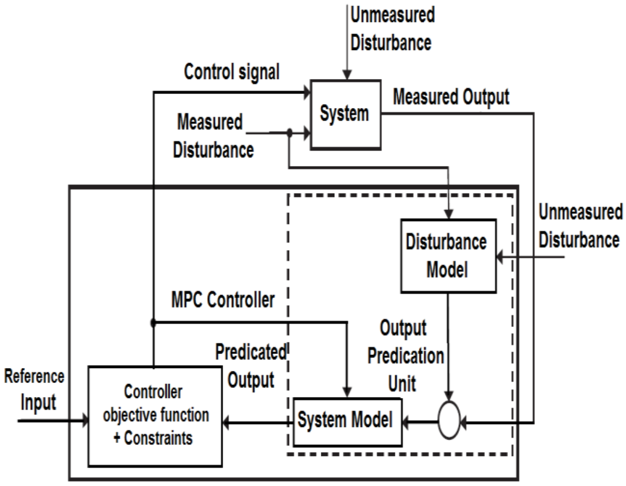

Fig. 8 General Structure of a MPC Algorithm

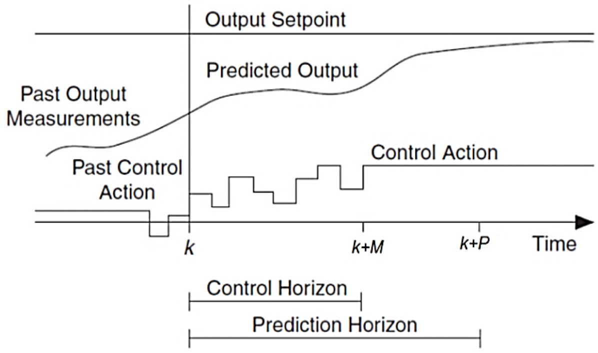

Fig. 9 Basic Concept for Model Predictive Control

THEORYOF FOPID

The FOPID controller is a public law of the PID controller. The following equation describes the transfer function of FOPID controller:

$$C(s) = k_p + \frac{k_i}{s^{\lambda}} + k_d s^{\mu} \tag{25}$$

Where

k_p The proportional constant

k_i The integration constant

k_d The differentiation constant

λ and μ Positive real numbers in the range [0 2]

The performance of the FOPID controller can improve by optimal setting of its parameters. This paper uses the GA for optimal tuning of FOPID controller parameters.

The fractional order operator $S^{\lambda \text{ or } \mu}$ is derived by Oustaloup's method utilizes a band-pass filter established with frequency- domain response. The Oustaloup' algorithm can derive the transfer function with fractional order operator S^{λ} as follows:

$$G_f(s) = K \prod_{k=-N}^{N} \frac{s+\omega_k'}{s+\omega_k} \tag{26}$$

Where, the zeros, poles and the gain is defined as:

$$\omega_k' = \omega_b \left(\frac{\omega_h}{\omega_b} \right)^{\frac{k+N+0.5(1-\lambda)}{2N+1}} \tag{27}$$

$$\omega_k = \omega_b \left(\frac{\omega_h}{\omega_b} \right)^{\frac{k+N+0.5(1+\lambda)}{2N+1}} \tag{28}$$

$$K = \left(\frac{\omega_h}{\omega_b}\right)^{-\frac{\lambda}{2}} \prod_{k=-N}^{N} \frac{\omega_k}{\omega_k'} \tag{29}$$

In simulation, the frequency range limits is defined as: ω ϵ [ω_b ω_h] and ω_b= 0.001, ω_h=1000, N=2. More detail is available in [24].

IMPERIALISTCOMPETITIVEALGORITHM

The ICA is a new developmental optimization algorithm established based on the socio-political process. It has emphasized its excellent performance, such as faster convergence and good achievement of global minimum. In this algorithm, every individual of the population is represent a country and known as:

$$Conntry = [\, C_1 . C_2 . \dots \dots . C_n \,] \tag{30}$$

Where n-dimensional optimization problem and the associated cost of a country is determined by:

$$C_n = f_{cost}^{(imp\,.n)} - \max_i (f_{cost}^{(imp\,.i)}) \tag{31}$$

Where f_{cost} is the value of the cost function of the controller parameters which means the related objective function and $f_{cost}^{(imp\,.n)}$ is the cost of the n^{th} imperialist. According to their power or naturalized cost, the initial colonies are moved between empires and for the n^{th} empire it will be as follows:

$$NC_n = round\left[\left|\frac{C_n}{\sum_{i=1}^{N_{imp}} c_i}\right| . N_{col}\right] \tag{32}$$

Where NC_n is the initial number of the colonies associated with the n^{th} empire which chosen randomly between the colonies and the number of imperialists. It is known as N_{imp} and N_{col} respectively. After creating initial empires, their colonies start pushing toward the imperialist country. Figure 10 demonstrates this development in which a colony pushes toward the imperialist by uniformly moved among 0 and $\lambda \times d$:

$$\bar{X}_{new} = \bar{X}_{old} + U(0.\lambda \, x \, d) x \, V \tag{33}$$

Where d is the separation among colony and imperialist and λ is a control parameter. V is a vector with a unit length. To spread the space about the imperialist, a random value of variation, θ is added to the direction of movement displays in (34):

$$\theta = U(-\gamma \,. +\gamma\,) \tag{34}$$

Where γ is an arbitrary number that changes the random area of colonies about the imperialist. If this repositioning operation creates a colony with better fitness, the locations of the imperialist and the colony are changed and the new position with the lower cost turns into the imperialist.

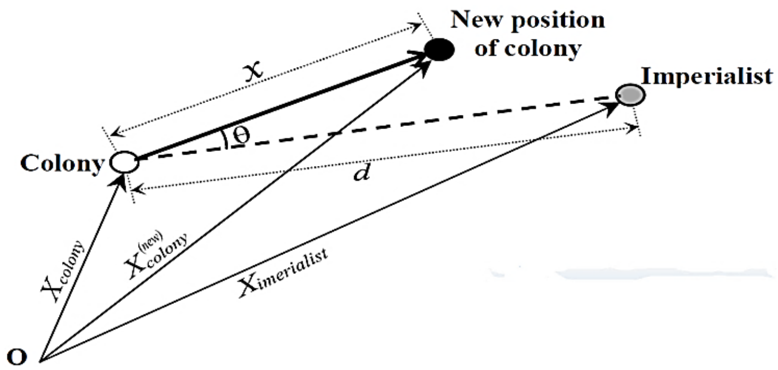

Fig. 10 Motion of colonies toward their relevant imperialist

In this algorithm, the empire power is determined by adding of the power of imperialist state to a colonies average power as follows:

$$TC_n = f_{cost}^{(imp\,.n)} + \zeta . \frac{\sum_{i=1}^{NC_n} f_{cost}^{(col\,.i)}}{NC_n} \tag{35}$$

Where TC_n is the full estimate of the n^{th} empire and ζ is a number greater than zero and the naturalized total cost is calculated by:

$$NTC_n = TC_n - \max_i (TC_i) \tag{36}$$

Where NTC_n is the naturalized total cost of the n^{th} empire. Having the naturalized total cost, the ownership probability of every empire is calculated by:

$$P_n = \left|\frac{NTC_n}{\sum_{i=1}^{N_{imp}} NTC_i}\right| \tag{37}$$

Any empire that can't pass in imperialist competition and isn't able to increase its power will be cancelled. The concerning colonies will be spread between the other empires. The above methodology result that all the countries converge to a state in which there produce only one empire represent the world and its colonies represent all the other countries. The flowchart of the ICA is investigated in Fig. 11. More details can be found in [21-23].

The best parameters of ICA program are selected with trial and error method. Number of initial countries 100,Number of Initial Imperialists 2,Number Of decades 200, Revolution Rate 0.3 (Revolution is the process in which the socio-political characteristics of a country change suddenly),Assimilation Coefficient 2 (assimilation coefficient is shown by beta), Assimilation Angle Coefficient 0.5 (assimilation angle coefficient is shown by gama), Total Cost of Empire 0.02 (Total Cost of Empire = Cost of Imperialist + Zeta * mean (Cost of All Colonies)), Damp Ratio 0.99, Uniting Threshold = 0.02 (The percent of Search Space Size, which enables the uniting process of two Empires), zarib = 1.05 (Zarib is used to prevent the weakest empire to have a probability equal to zero),alpha = 0.1 (alpha is a number in the interval of [0 1] but alpha<<1. alpha denotes the importance of mean minimum compare to the global minimum).

The computational efficiency of the optimization algorithms plays a critical role in tuning the online controller for a real control system so I used a computer with processor Intel(R) core(TM) i3 -6006U CPU @ 2.00 GHZ 2.00 GHZ, and Installed memory (RAM) 4.00 GB and system type 64-bit operating System.

TURBO-GENERATORSYSTEMBASEDON MPC

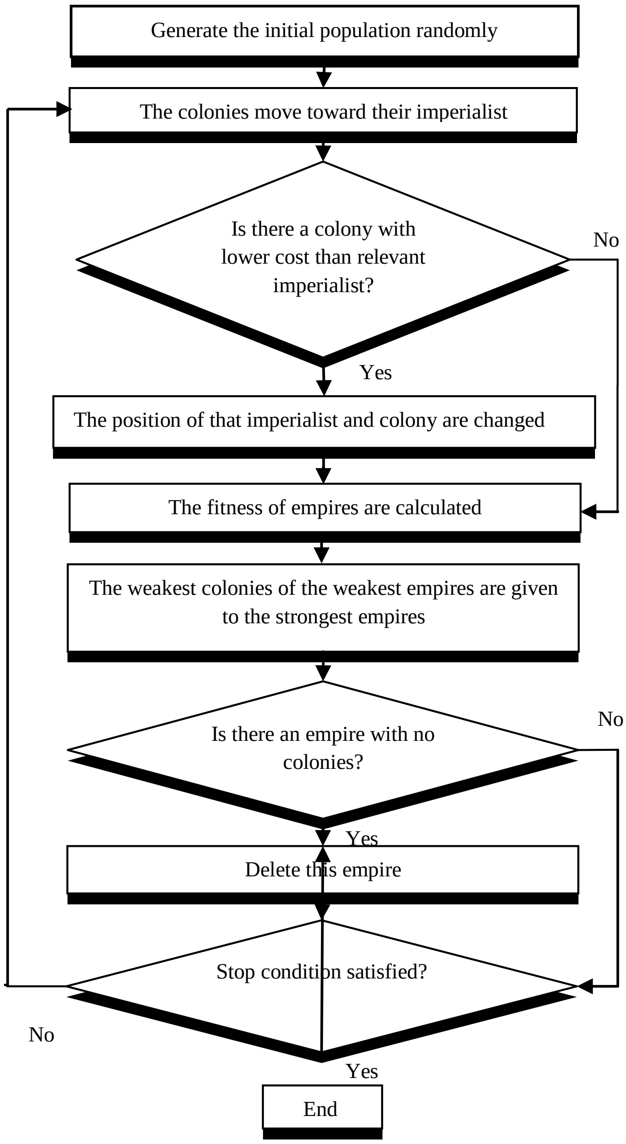

Fig. 11 Flowchart of the ICA

In the proposed turbo-generator system [25], there are two MPC controller required to control the voltage and the power of the generator as shown in Fig. 12. The proposed configuration is done in Matlab Simulink utilizing MPC toolbox. The configuration is started by determining the linear time invariant (LTI) model of the plant to be controlled. These LTI models act as discrete state-space models. The ICA is devoted for searching the MPC parameters in order to minimize the following objective function:

$$J = \int_{t=0}^{t=t_f} t[\,|V_{ref} - V_t(t)| + |P_{ref} - P_t|\,] \qquad (38)$$

The optimal parameters of ICA-based FOPID and ICA-based MPC are listed in Table 1 with the objective functions values. From Table 1, it is clear the ICA-based MPC has the minimum objective value.

Table -1 Controller parameters and the objective function (J)

	ICA-based MPC	GA-based MPC	GA-based FOPID
MPC_1 parameters	T_{s1}= 0.7462, P_1 = 205, M_1 = 100 R_1 = 1, Q_1= 0.1	T_{s1}= 1.622, P_1 = 184, M_1 = 52 R_1 = 0.6490, Q_1= 7.8640	K_{p1}=*0.5099*, K_{i1}=*80*, K_{d1}=*40*, λ_1=0.99, μ_1=0.3757
MPC_2 parameters	T_{s2}= 0.4694, P_2 = 224, M_2 = 7 R_2 = 0.007, Q_2= 40	T_{s2}= 0.5060, P_2 = 92, M_2 = 20 R_2 = 0.116, Q_2=3.515	K_{p2}=*0.6*, K_{i2}=*0.001*, K_{d2}=*0.1*, λ_2=0.3009, μ_2=0.0835
Objective function (J)	0.88	2.0969	4.1292

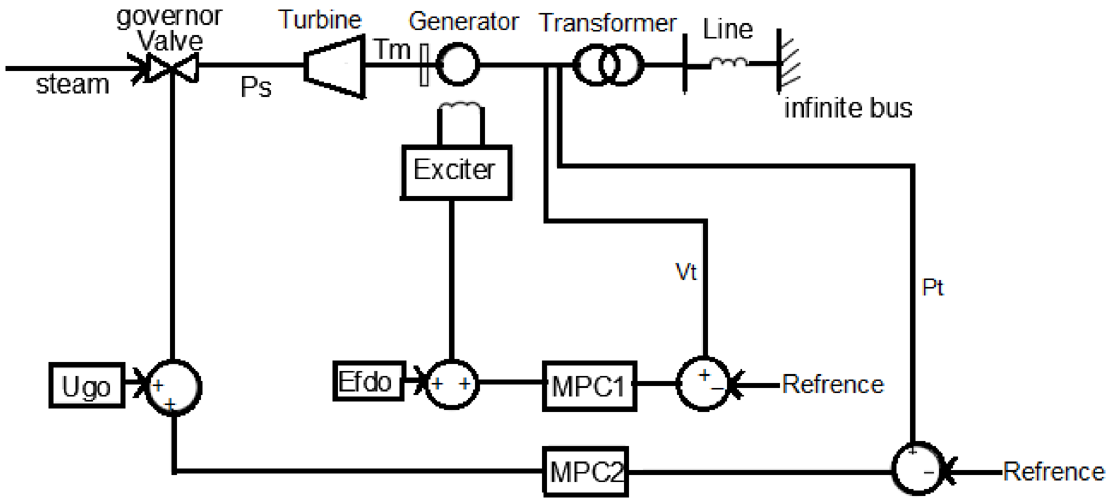

Fig. 12 Turbo-Generator System Controlled by MPC

RESULTS AND DISCUSSION

Effect of Three Phase Short Circuit Disturbance with 120ms Fault Time

This test is provided to show the feasibility of designed MPC in attenuating heavy exogenous disturbance represented by three phase short circuit that is applied at the infinite bus and lasting for 120 milliseconds. In the beginning, the nonlinear model of a single machine infinite bus power system reference values is set to V_{ref} = 1.064 p.u and P_{ref} = 0.8 p.u. Once the system has settled down to its steady state, a 120-ms balanced three phase short circuit is applied (t = 1s) at the terminal of the machine. Figure 13 shows the system time response of the system terminal voltage and power driven by different control methods. As shown in Fig. 13, oscillations are presented in V_t and P_t, the system regains its stability after a few seconds. It is clear that the ICA-based MPC has the best performance oscillations compared to GA-based MPC and GA-based FOPID controller.

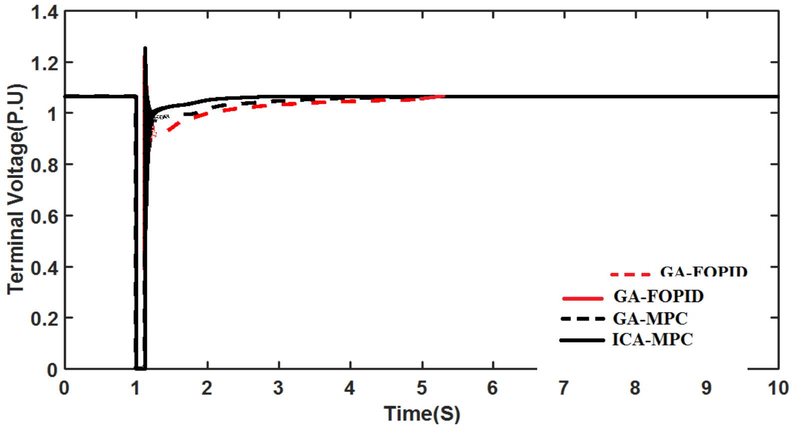

(a)

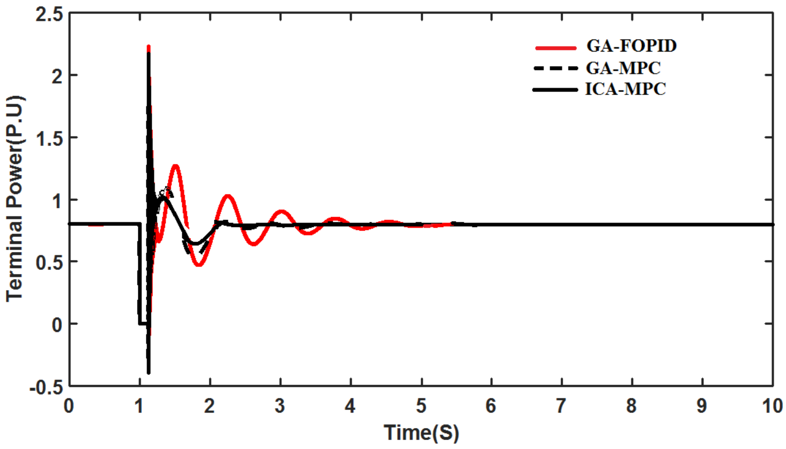

(b)

Fig. 13 Effect of three phase short circuit disturbance with 120ms (a) Voltage terminal response, (b) Power terminal response

Effect of Three Phase Short Circuit Disturbance with 200ms Fault Time

This test is carried out to show the performance of MPC in case of increasing the three phase short circuit duration at the infinite bus and lasting for 200 milliseconds. As shown in Fig. 14, the oscillations are presented in V_t and P_t, the system regains its stability after a few seconds. It is clear that ICA-based MPC show improved performance summarized in faster response with fewer oscillations than GA-based MPC and GA-based FOPID.

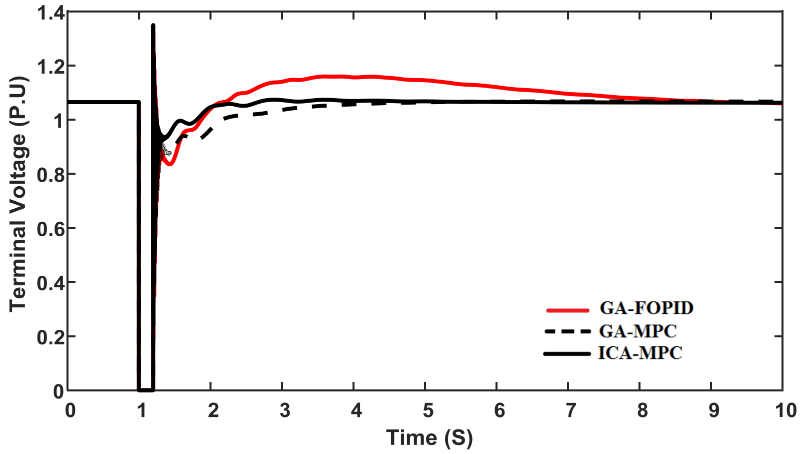

(a)

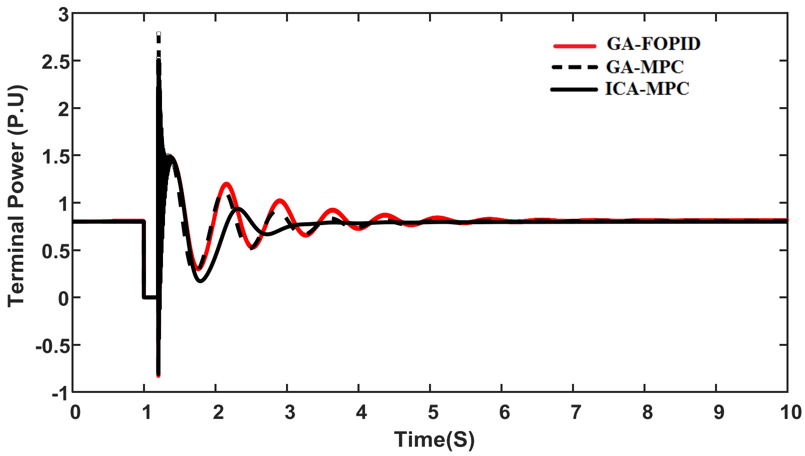

(b)

Fig. 14 Effect of three phase short circuit disturbance with 200ms (a) Voltage terminal response, (b) Power terminal response.

Effect of Load Variation By 15% Increase with 120ms disturbance Time

In this test, a 15% increase in load with 120ms disturbance time t_d is applied. As shown in Fig. 15, oscillations are presented in V_t and P_t , the system regains its stability after a few seconds It is clear that the system response with ICA-based MPC more damped and faster response (1 s for ICA- based MPC, 3s for GA-MPC and 5s for GA-FOPID) than GA-based MPC and GA-based FOPID controller.

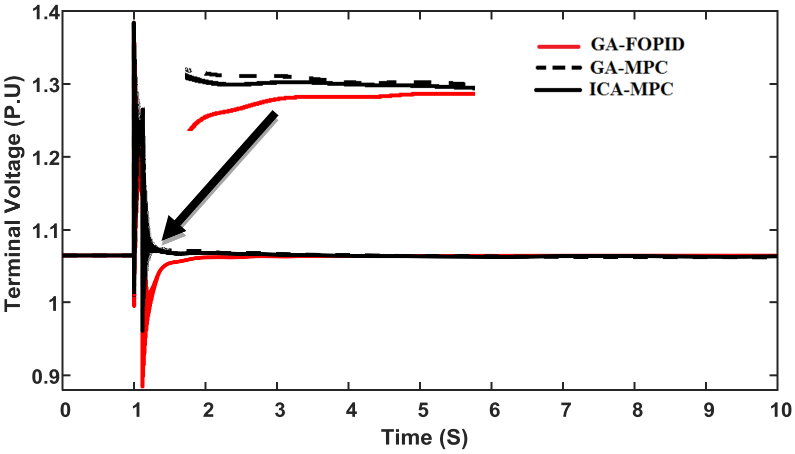

(a)

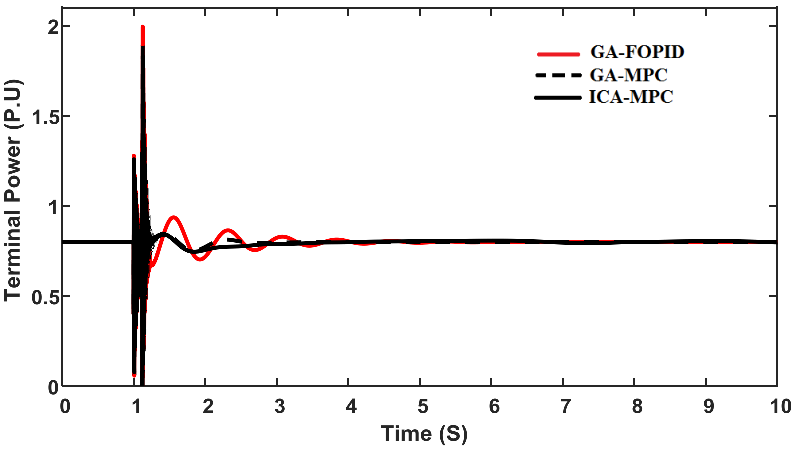

(b)

Fig. 15 Effect of load variation by 15% increase with T_d =120ms (a) Voltage terminal response, (b) Power terminal response

Effect of Mechanical Power input Variation by 15% Decrease with 120ms Disturbance Time

In this test, a 15% decrease in mechanical input power with 120ms disturbance time is applied. As shown in Fig. 16, oscillations are presented in V_t and P_t, the system regains its stability after a few seconds. It is clear that ICA-based MPC show improved performance summarized in faster response (1 s for ICA- based MPC, 3 s for GA-MPC and 5 s for GA-FOPID) with fewer oscillations than GA-based MPC controller and GA-based FOPID.

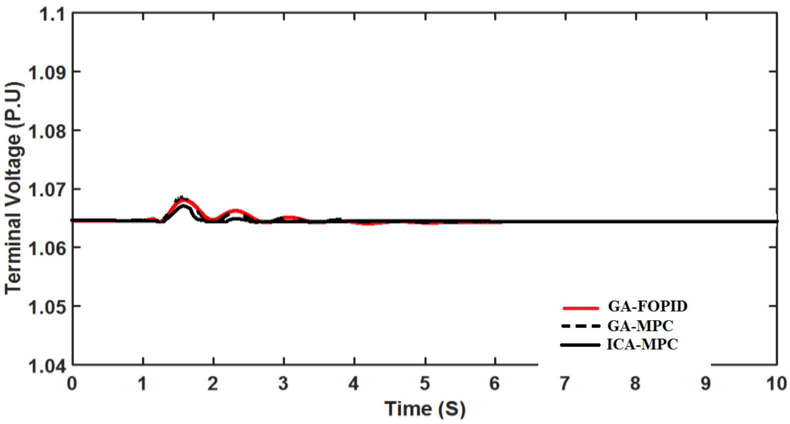

(a)

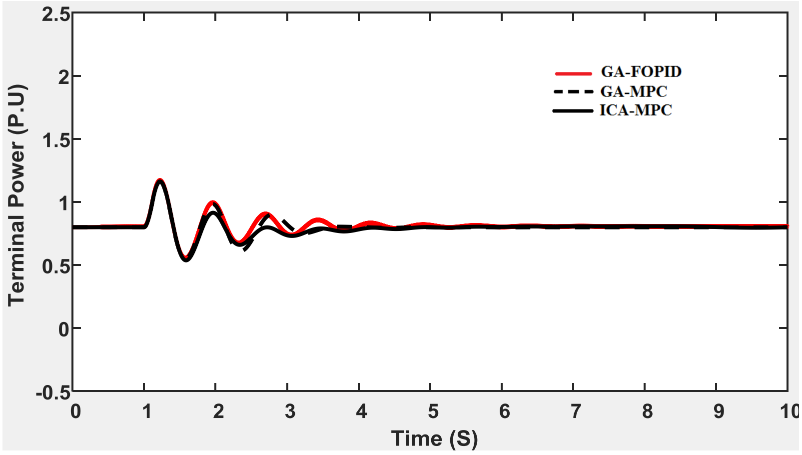

(b)

Fig. 16 Effect of mechanical power variation by 15% decrease with T_d =120ms (a) Voltage terminal response, (b) Power terminal response

Effect of Mechanical Power input Variation by 15% Increase and Load Variation by 15% Decrease with 120ms Disturbance Time

In this test a 15% increase in mechanical input power and 15% decrease in load with 120ms disturbance time are applied. As shown in Fig. 17, oscillations are presented in V_t and P_t, the system regains its stability after a few seconds. It is clear that MPC show improved performance summarized in faster response (3 s for ICA- based MPC, 4 s for GA-MPC and 7 s for GA-FOPID) with fewer oscillations than GA-FOPID and GA- MPC.

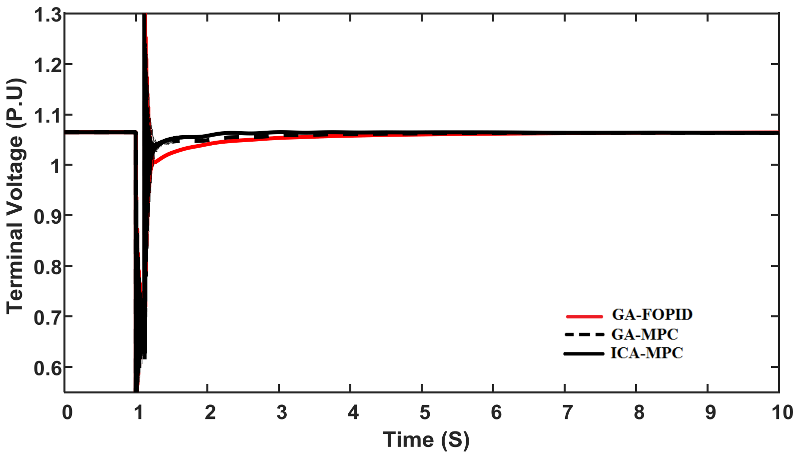

(a)

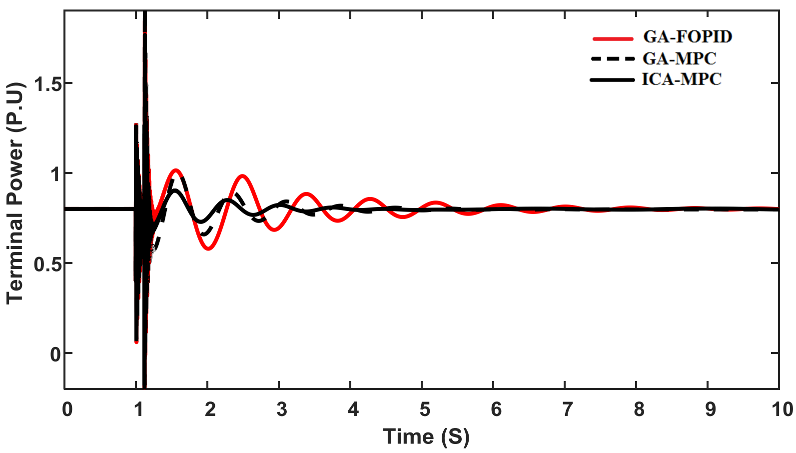

(b)

Fig. 17 Effect of mechanical power variation by 15% increase and voltage variation by 15% decrease with 120ms (a) Voltage terminal response, (b) Power terminal response

Robustness Study

This test is carried out to confirm the robustness of the proposed ICA-based MPC design when occurring system parameter uncertainties. The inertia and field resistance coefficient are changed around its nominal value (H, R_{fd}) by ±20%, i.e. (H, R_{fd}) ϵ [(0.8 (H, R_{fd}) 1.2 (H, R_{fd})]. As shown in Fig. 18, the proposed ICA-based MPC can damp the system oscillation under system uncertainties with a non-significant change in the system response.

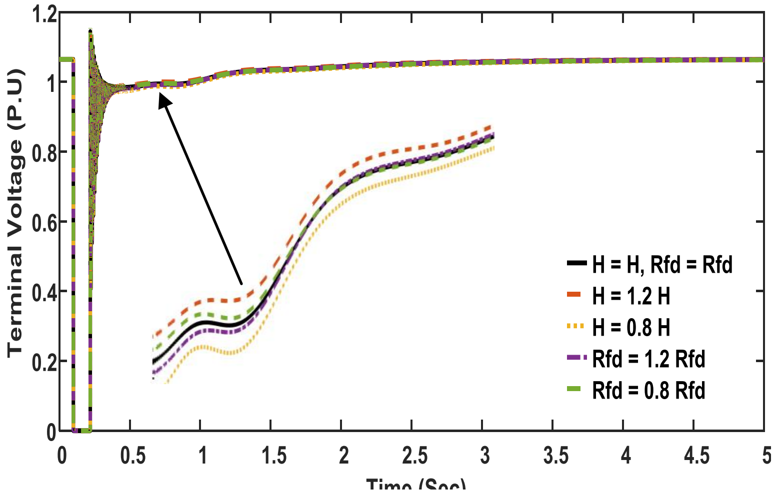

(a)

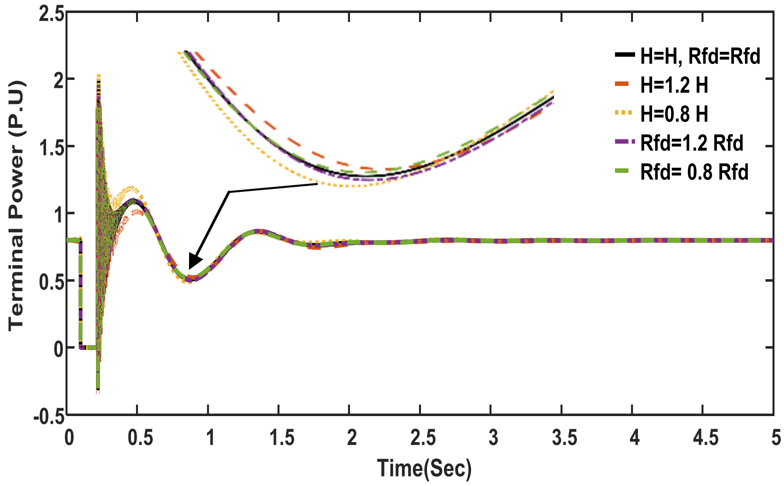

(b)

Fig. 18 System Response Subject to Robustness Study *(*a) Voltage terminal response, (b) Power terminal response

CONCLUSION

In this paper, the parameters of model predictive control in a turbo-generator system are optimized by ICA to overcome the system nonlinearities. Moreover, overcome the system parameter uncertainties, stabilization of terminal voltage and terminal power of the turbo-generator system are achieved. In addition, incorporating transport short circuit and mechanical and electrical variation are carried out. A comparison between the proposed ICA-based MPC, GA-based MPC, and GA-based FOPID controllers has demonstrated the superiority of ICA-based MPC design. The can overcome the system nonlinearities and transport short circuit and mechanical and electrical variation. Consequently, the proposed design can ensure the system stability when load perturbations are increased, excessive short circuit, mechanical, and electrical variation. Simulation results have been investigated to confirm on the robustness of the proposed design in the case of system parameters uncertainties.

APPENDIX

ω_o=400*atan(1); H=3.25; R_{fd}=1.5*0.0015; R_{kq}=0.038; X_{ad}=1.86; X_{aq}=1.77; X_{fd}=1.97; X_d=2; X_q=1.91; X_{kd}=1.936; X_{kq}=1.9; K_d=0; X_t=0.101; R_l=0.0025/2; X_l=0.352/2; R_a=0.005; R_l=0; R_t=0; R_e=0; X_e=X_l+X_t; K=0; F_{hp}=0.24; F_{ip}=0.34; F_{lp}=0.42; P_0=1.2; X_{fkd}=X_{ad}; X_{akd}=X_{ad}; X_{akq}=X_{aq}; T_{mv}=.1; T_{iv}=.1; T_{hp}=.3; T_{rh}=1; T_{ip}=.3; T_{lp}=.72; F_{hp}=.24; F_{ip}=.34; F_{lp}=.42; ω= ω_o;

A=[X_{fd} -X_{ad} X_{ad};X_{ad} -X_d X_{ad};X_{ad} -X_{ad} X_{kd}]; Y=inv(A);

B=[-X_q X_{aq};-X_{aq} X_{kq}]; D=inv(B);

$c_1=\omega_o/(2*H)$; $d_{11}=D(1,1)$; $Y_{22}=Y(2,2)$; $c_2=c_1*(Y_{22}-d_{11})$; $d_{12}=D(1,2)$; $c_3=c_1*-d_{12}$; $Y_{21}=Y(2,1)$; $c_4=c_1*Y_{21}$; $Y_{23}=Y(2,3)$; $c_5=c_1*Y_{23}$; $c_6=-c_1*K$; $c_7=\omega_o*R_{fd}/X_{ad}$; $Y_{11}=Y(1,1)$; $c_8=-W_o*R_{fd}*Y_{11}$; $Y_{12}=Y(1,2)$; $c_9=-\omega_o*R_{fd}*Y_{12}$; $Y_{13}=Y(1,3)$; $V_b=0.932$; $c_{10}=-\omega_o*R_{fd}*Y_{13}$; $c_{11}=\omega_o*V_b$; $c_{12}=W_o*(R_a)*Y_{21}$; $c_{13}=\omega_o*(R_a)*Y_{22}$; $c_{14}=\omega_o*(R_a)*Y_{23}$; $Y_{31}=Y(3,1)$; $c_{15}=-\omega_o*R_{kd}*Y_{31}$; $c_{16}=-\omega_o*R_{kd}*Y(3,2)$;$c_{17}=-\omega_o*R_{kd}*Y(3,3)$;$c_{18}=\omega_o*(R_a)*D(1,1)$; $c_{19}=\omega_o*(R_a)*D(1,2)$; $c_{20}=-\omega_o*R_{kd}*D(2,1)$; $c_{21}=-\omega_o*R_{kd}*D(2,2)$;

REFERENCES

[1]. Andreev, M., Borovikov, Y., Gusev, A., Sulaymanov, A., Ruban, N., Suvorov, A., ... & Králík, T, Application of hybrid real-time power system simulator for research and setting a momentary and sustained fast turbine valving control, IET Generation, Transmission & Distribution,2017, 12(1), 133-141.

[2]. Franck, C. M, HVDC circuit breakers: A review identifying future research needs. IEEE Transactions on Power Delivery, 2011, 26(2), 998-1007.

[3]. Øyvang, T., Hegglid, G. J., & Lie, B, Models of synchronous generators with excitation system, for transient power system studies, IFAC-PapersOnLine,2018, 51(2), 91-96.

[4]. Bartlett, J. P., Gibbard, M. J., & Woodward, J. L, Performance of a 5 kVA synchronous generator with an optimal excitation regulator. In Proceedings of the Institution of Electrical Engineers IET Digital Library, 1973, 120(10), 1250-1256.

[5]. Franklin, G. F., Powell, J. D., & Workman, M. L, Digital control of dynamic systems, 1998 (Vol. 3). Menlo Park, CA: Addison-wesley.

[6]. Wang, Z., & Lemmon, M, Using decentralized secondary controllers to improve transient stability of generators in lossy power networks. IEEE In American Control Conference (ACC), 2016, 5903-5908.

[7]. Nazaruddin, Y. Y., & Unbehauen, H, Design of a multivariable state-space adaptive controller, and its application to a turbogenerator pilot plant. Control Engineering Practice, 1996, 4(5), 699-704.

[8]. Sharaf, M. M., & Hogg, B. W., Identification and control of a laboratory model turbogenerator. International Journal of Control, 1980, 31(4), 723-739.

[9]. Sharaf, S. M., & Serag, A. M, Practical identification and PI optimal controller of a laboratory drive system, International Journal of Control, 1995, 62(3), 511-526.

[10]. Salgado, I., Mera, M., & Chairez, I., Suboptimal adaptive control of dynamic systems with state constraints based on Barrier Lyapunov functions. IET Control Theory & Applications, 2018, 12(8), 1116-1124.

[11]. Venayagamoorthy, G. K., Wunsch, D. C., & Harley, R. G, Comparison of heuristic dynamic programming and dual heuristic programming adaptive critics for neurocontrol of a turbogenerator, IET Control Theory & Applications, 2002, 10(8), 200-210.

[12]. Mahmoud, M., Dutton, K. and Denman, M, Design and simulation of a nonlinear fuzzy controller for a hydropower plant, Electric Power Systems Research, 2005, 73(2), 87-99.

[13]. Dobrescu, M and Kamwa, I,A New Fuzzy Logic Power System Stabilizer Performances, IEEE PES Power systems Conference and Exposition, 2004, v 2, pp. 1056-1061.

[14]. Nallathambi, N. and Neelakantan, P.N, Fuzzy Logic Based Power System Stabilizer, Tech An International Multi Topic Conference, 2004, V 04, 68-73.

[15]. Qin, S. J., & Badgwell, T. A, A survey of industrial model predictive control technology. Control engineering practice, 2004, 11(7), 733-764.

[16]. Ersdal, A. M., Imsland, L., & Uhlen, K., Model predictive load-frequency control, IEEE Transactions on Power Systems, 2016, 31(1), 777-785.

[17]. Wang, T., Gao, H., & Qiu, J, A Combined Adaptive Neural Network and Nonlinear Model Predictive Control for Multirate Networked Industrial Process Control, IEEE Trans. Neural Netw. Learning Syst, 2016, 27(2), 416-425.

[18]. Liu, X., Kong, X., & Lee, K. Y, Distributed model predictive control for load frequency control with dynamic fuzzy valve position modelling for hydro–thermal power system, IET Control Theory & Applications,2016 10(14), 1653-1664.

[19]. Bernard, M. Z., Mohamed, T. H., Qudaih, Y. S., & Mitani, Y, Decentralized load frequency control in an interconnected power system using Coefficient Diagram Method, International Journal of Electrical Power & Energy Systems,2014, 63, 165-172.

[20]. Mayne, D. Q, Model predictive control, Recent developments and future promise. Automatica, 2014, 50(12), 2967-2986.

[21]. Xing, B., & Gao, W. J, Imperialist competitive algorithm. In Innovative computational intelligence: A rough guide to 134 clever algorithms, Springer, Cham, 2014, 203-209.

[22]. Atashpaz-Gargari, E., & Lucas, C, Imperialist competitive algorithm: an algorithm for optimization inspired by imperialistic competition. In Evolutionary computation, CEC IEEE Congress, 2007, 4661-4667.

[23]. Shabani, H., Vahidi, B., & Ebrahimpour, M, A robust PID controller based on imperialist competitive algorithm for load-frequency control of power systems, ISA transactions, 2013, 52(1), 88-95.

[24]. Taher, S. A., Fini, M. H., & Aliabadi, S. F, Fractional order PID controller design for LFC in electric power systems using imperialist competitive algorithm, Ain Shams Engineering Journal, 2014, 5(1), 121-135.
[25]. Mai, H. H, Fuzzy Neural Network for Control of Turbo-generator System, Master of Science Thesis, Faculty of Engineering, Helwan University, 2010.